PHILOSOPHICAL TRANSACTIONS OF THE ROYAL SOCIETY A MATHEMATICAL, PHYSICAL & ENGINEERING SCIENCES

Stability Predictions through a Succession of Folds

J. M. T. Thompson

Phil. Trans. R. Soc. Lond. A 1979 **292**, 1-23
doi: 10.1098/rsta.1979.0043

STABILITY PREDICTIONS THROUGH A SUCCESSION OF FOLDS

By J. M. T. THOMPSON
Department of Civil Engineering, University College, London, U.K.

(*Communicated by E. C. Zeeman, F.R.S. – Received* 17 *August* 1978)

CONTENTS

PAGE

Introduction 2

I. General analysis 2
1. Formulation 2
2. The conjugate theorem 3
3. Perturbation equations 6
4. Normal equilibrium state 7
5. Critical equilibrium state 8

II. The concept of internal stability 9
6. Extreme forms of loading 9
7. Practical loading arrangements 10
8. The conjugate property 11
9. Relations between internal and external stability 11
10 Internal stability with external instability 13

III. Applications 13
11. A pinned arch 13
12. A shallow spherical dome 14
13. Thermodynamics of a hot stellar mass 15
14. Gravitational collapse of a massive cold star 16
15. Bifurcations under rigid loading 19

Concluding remarks 20

Appendix 21

References 22

For a discrete, or discretized, conservative gradient system, such as is envisaged in catastrophe theory and arises throughout the physical sciences, it is often necessary to assess the stable regions of an equilibrium path that exhibits a succession of folds. At each fold the degree of instability changes by one, so that as the system evolves from a region of known stability the first fold must represent a loss of stability. At a second fold, however, it is not clear whether the system is suffering a further loss, as we shall see in some examples, or is regaining its original stability as is more common in elasticity. A

new theorem involving a conjugate parameter allows all such stability changes to be readily assessed on the basis of the form of the equilibrium paths themselves.

The application of the general theory to the external and internal stabilities of an elastic structure under dead and rigid loading is demonstrated. Under the former, the load is the control parameter and the corresponding deflection plays the role of the conjugate parameter, while in a direct analysis of rigid loading these roles are reversed. A supplementary study of rigid loading which uses Lagrange multipliers supplies further theorems relating the dual concepts of external and internal stability.

The use of the theorems is demonstrated in the buckling of elastic arches and shallow domes, and in the incipient gravitational collapse of a massive cold star. The possible stabilization of bifurcations by rigid loading is examined, and shows how the results can also be of value in bifurcational instabilities.

Introduction

In the physical sciences, and particularly in elasticity and astrophysics, it is often necessary to assess the stability of an equilibrium path generated by the slow scan of a single fundamental control parameter. Such a path might for example have been determined numerically by simply solving the statical equilibrium equations on a computer.

Now for a discrete conservative system, catastrophe theory (Thom 1975; Zeeman 1977; Poston & Stewart 1978) shows that the only structurally stable way in which a change of stability can arise is at a fold, where the equilibrium path takes a locally extreme value of the single control parameter. The only other way in which a change of stability can arise is at a point of bifurcation involving the intersection with a second path, as guaranteed by a recently proved basic theorem of elastic stability.

Focusing attention on the generic folds, we often need to deduce the stable regions of a continuous equilibrium path exhibiting a succession of folds. Very often physical reasoning will guarantee the stability of one end of this path, and we are left with the problem of assessing possible stability changes as we progress away from this region. At each fold the degree of instability (the number of negative stability coefficients) changes by one, and so a fold terminating our region of known stability must imply a *loss* of stability. At a subsequent fold, however, it is not clear whether the system is suffering a further loss, or, conversely, is regaining its original stability. Both alternatives are indeed possible as we shall demonstrate in some illustrations.

A new conjugate theorem established by Katz (1978) to examine the stability transitions of isothermal stellar spheres allows all such stability changes to be assessed by using a plot of the control parameter against an energy derivative. This theorem is here related to the energy transformations of the fold catastrophe and specialized to deal with the dead and rigid loading of elastic structures where the conjugate energy derivative is related to the corresponding deflexion and the passive constraining load respectively.

The general theory is finally applied to the buckling of elastic arches and domes, the gravitational instability of a massive cold star, and the prediction of internal stability changes at distinct points of bifurcation.

I. General analysis

1. *Formulation*

Consider a general system governed by a potential energy function $V(Q_i, \Lambda)$, where the Q_i are a set of n generalized coordinates and Λ is a single controlled parameter. Such a system has been

extensively studied in nonlinear elasticity (Thompson & Hunt 1973), and in the thermodynamical applications of astrophysics V can be taken as the negative of the entropy. The normal equilibrium and stability conditions are assumed to hold, and the use of a set of generalized coordinates implies some standard discretization of continuous systems.

In the buckling of engineering structures the control parameter is often a load appearing linearly in the potential energy, and when this linearity holds we shall write Λ as P, and V as

$$V = U(Q_i) - P\mathscr{E}(Q_i). \tag{1}$$

Here $U(Q_i)$ is a generalized strain energy and P can be viewed as the magnitude of a generalized force acting through the corresponding deflexion $\mathscr{E}(Q_i)$.

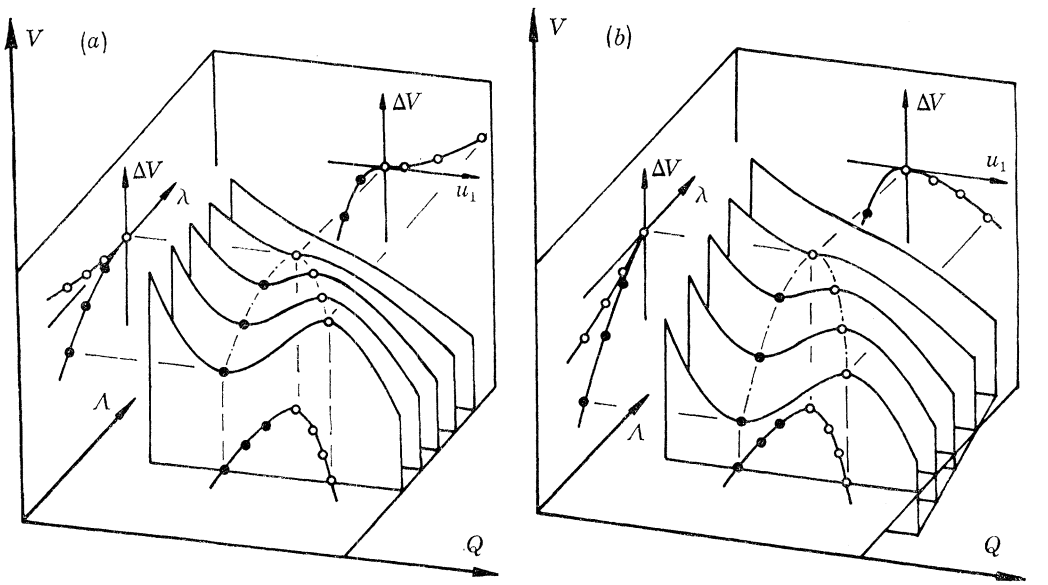

FIGURE 1. Two forms of the energy transformations in the fold catastrophe. (*a*) $V'^{G} = 0$; (*b*), $V'^{G} > 0$.

2. *The conjugate theorem*

It is a simple observation from catastrophe theory that the energy surface of a fold (or limit point) has the topological form of the equilibrium surface of a cusp (or distinct symmetric point of bifurcation).

This is illustrated in figure 1, which contains two schematic representations of an energy surface of a fold, the three dimensions of the pictures representing an activity subspace of the real $(n+2)$ dimensional space spanned by Q_i, Λ and V. In seeking a stable equilibrium state the system must here find a locally minimum value on the constant Λ curves. Incremental fixed axes measured from the critical point represent ΔV, the change in V from the critical value, λ the change in Λ from the critical value, and u_1 the local principal coordinate that participates in the instability.

The chain-dotted equilibrium path reaches a maximum value of Λ at the critical point, and the stability transition is indicated by the circles. A solid circle denotes an equilibrium state that is stable with respect to u_1 and an open circle denotes an equilibrium state that is unstable with respect to u_1. Notice that we are here talking only about the stability *with respect* to u_1, which is the principal coordinate (associated with a diagonalized energy quadratic) that is involved in the instability. The whole of the drawn path might be either stable or unstable with respect to any other local principal coordinate u_t.

Projections of the equilibrium path are indicated, and we observe in particular that the V against Λ plot exhibits the two-thirds power law cusp familiar as the stability boundary (or imperfection–sensitivity diagram) of the cusp catastrophe.

Now since at any Λ level we have an arbitrary choice of energy datum, the constant Λ curves can be sheared like a stack of playing cards without altering any physical characteristics of the system. In particular we could if we wished adjust the value of $V'^{\mathrm{C}} = \partial V/\partial\Lambda|^{\mathrm{C}}$, where the superscript C denotes evaluation at the critical equilibrium state. If V'^{C} is zero the cusp is aligned horizontally as shown in the left-hand diagram, while if V'^{C} is non-zero the projected cusp is tilted or inclined as in the right hand diagram. Typically or generically the cusp will of course be tilted, and we notice that the form of the V against Q projection is significantly different for the two cases.

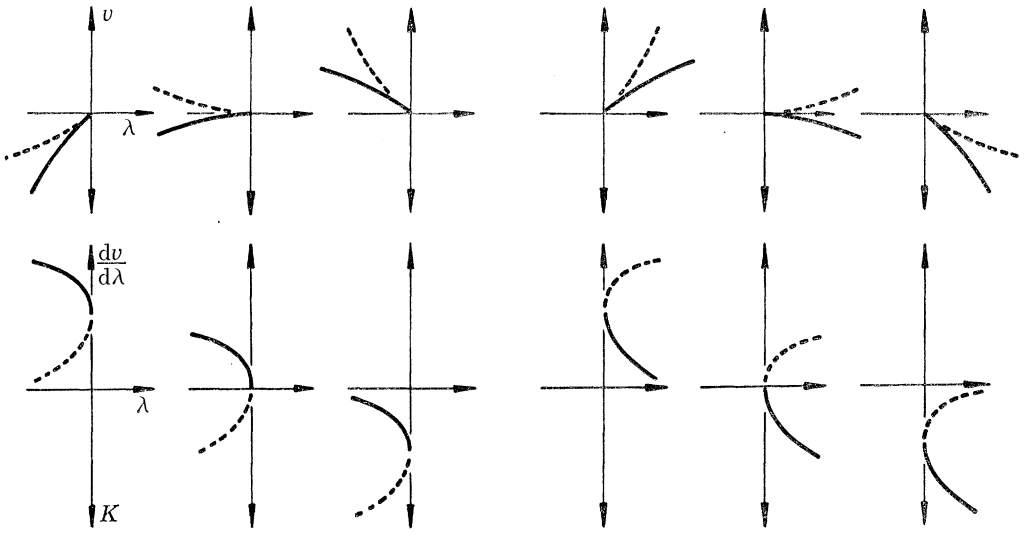

FIGURE 2. Six possible forms of the fold showing the energy-control cusps and the corresponding plots of the conjugate parameter against the control.

Now if we have in front of us just the Λ against Q projection of such a fold, we cannot in general deduce the direction of the stability loss, since a maximum might be either stable to the right or stable to the left. However, if we have in front of us the projected V against Λ graph it is clear that the upper limb represents equilibrium states that are unstable with respect to u_1 while the lower limb represents equilibrium states that are stable with respect to u_1.

In some important classes of problems, Katz observed that there exists a *conjugate parameter* K which we can here define on the equilibrium path as the negative of $\mathrm{d}V/\mathrm{d}\Lambda$; this total derivative, being the slope of the V against Λ projection, should not be confused with $V' = \partial V/\partial\Lambda$. Now if we plot K against Λ the projected cusp is replaced by a smooth locally parabolic curve as illustrated by the possibilities of figure 2, and it is clear that the stability of the equilibrium path is governed by the sign of $\mathrm{d}K/\mathrm{d}\Lambda$ near the singularity. When this derivative is positive we have stability with respect to u_1 while when it is negative we have instability with respect to u_1. We should emphasize that this result is only true *close to the singularity* since the equilibrium path can, and frequently does, pass subsequently through a point of vertical tangency ($\mathrm{d}K/\mathrm{d}\Lambda = 0$) with a resulting change in sign but no change in stability.

This result has useful predictive value, and we cast it formally as a conjugate theorem:

THEOREM 1. *In the immediate vicinity of a fold catastrophe (or limit point) a positive/negative slope implies stability/instability with respect to the critical principal coordinate on a plot of the control parameter against the conjugate parameter.*

This result is illustrated in the two upper graphs of figure 3, which show two folds forming a typical hysteresis cycle as seen in the environment of a cusp catastrophe.

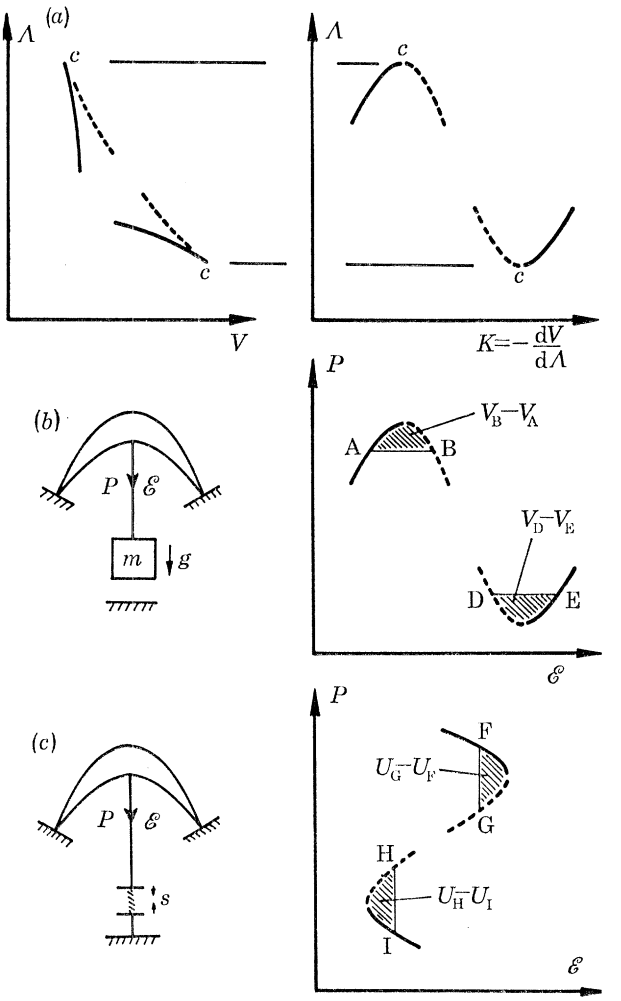

FIGURE 3. (*a*), two folds forming a typical hysteresis cycle for the general system; (*b*), two folds in the dead loading of a structure; (*c*), two folds in the rigid loading of a structure.

When we have a structure loaded by a generalized force P the area under the equilibrium path on a plot of P against $\mathscr{E}$ represents the strain energy of the system, U. We can use this fact to establish the corresponding theorems for dead and rigid loading.

When the loading is dead, the generalized force P is our control parameter, and the total potential energy $V = U - P\mathscr{E}$ is our potential function. This is illustrated in the central two pictures of figure 3 where P would equal mg, the product of the hanging mass and the acceleration due to gravity. The shaded areas can now be identified as the indicated changes in V, showing that

B and D must be the unstable states. Clearly $\mathscr{E}$ is now playing the role of the conjugate parameter and we can write the conjugate theorem for dead loading as:

THEOREM 2. *For an elastic structure under a generalized dead load, in the immediate vicinity of a fold catastrophe (or limit point) a positive/negative slope implies stability/instability with respect to the critical principal coordinate on a plot of the load against its corresponding deflexion.*

The rigid loading situation is illustated in the lower two pictures of figure 3. The corresponding deflexion $\mathscr{E}$ is now imposed, for example, by a rigid screw system, and becomes our controlled parameter; and the strain energy U, viewed now as a function of $n-1$ generalized coordinates and the displacement $\mathscr{E}$, becomes our potential function. The shaded areas can now be identified as the indicated changes in U, showing that with respect to the local critical principal co-ordinate u_1 the states G and H are unstable. Clearly $-P$ is now playing the role of the conjugate parameter, and we write the conjugate theorem for rigid loading as:

THEOREM 3. *For an elastic structure under a generalized rigid load, in the immediate vicinity of a fold catastrophe (or limit point) a positive/negative slope implies stability/instability with respect to the critical principal coordinate on a plot of the negative of the load against its corresponding deflexion.*

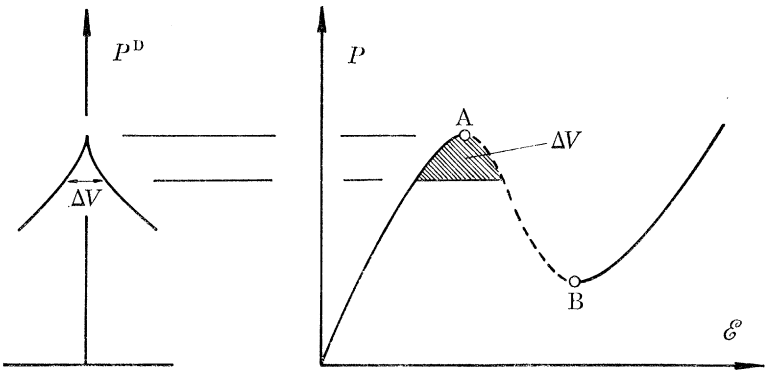

FIGURE 4. Imperfection-sensitivity to dynamic disturbances at a fold.

We can note finally in this section that the cusped form of the V–Λ or V–P projection of a fold catastrophe implies a two-thirds power law imperfection-sensitivity to dynamic energy disturbances, as illustrated in figure 4 for the dead loading of a structure. Here ΔV is now the magnitude of the energy disturbance *necessary* to cause collapse at a load level P^{D}. This magnitude may not be *sufficient*, since some of the energy input may be absorbed by other non-critical modes of vibration.

3. *Perturbation equations*

In order to study these results analytically, and to derive some further theorems, we now make a local perturbation analysis of our continuously folded equilibrium path. To do this we write the path parametrically as

$$Q_i = Q_i^{\mathrm{P}}(s), \quad \Lambda = \Lambda^{\mathrm{P}}(s), \tag{2}$$

where s is a suitable progress parameter, and we write the variation of V along the path as

$$V^{\mathrm{P}}(s) = V[Q_i^{\mathrm{P}}(s), \quad \Lambda^{\mathrm{P}}(s)]. \tag{3}$$

Setting $s = \Lambda$, we then define a *conjugate parameter*

$$K(\Lambda) = -\mathrm{d}V^{\mathrm{P}}/\mathrm{d}\Lambda. \tag{4}$$

To obtain local information about our equilibrium path P through an equilibrium state E we introduce a set of local incremental principal coordinates u_i tied to the state E. These coordinates vanish at E, and the energy written as $V(u_i, \Lambda)$ has a diagonal form with

$$V^{\mathrm{E}}_{ij} = 0 \quad \text{for} \quad i \neq j. \tag{5}$$

Here subscripts on V denote partial differentiation with respect to the corresponding principal coordinates u_i.

The equilibrium path, written now as $[u_i(s), \Lambda(s)]$ is characterized by the identity

$$V_i[u_j(s), \quad \Lambda(s)] = 0, \tag{6}$$

and by differentiating repeatedly with respect to s we generate the ordered equilibrium equations

$$V_{ij}\, u^{(1)}_j + V'_i\, \Lambda^{(1)} = 0, \tag{7}$$

$$[V_{ijk}\, u^{(1)}_k + V'_{ij}\, \Lambda^{(1)}]\, u^{(1)}_j + V_{ij}\, u^{(2)}_j + [V'_{ij}\, u^{(1)}_j + V''_i\, \Lambda^{(1)}]\, \Lambda^{(1)} + V'_i\, \Lambda^{(2)} = 0, \tag{8}$$

etc., where $$\Lambda^{(1)} = \mathrm{d}\Lambda/\mathrm{d}s, \quad \Lambda^{(2)} = \mathrm{d}^2\Lambda/\mathrm{d}s^2, \quad \text{etc.} \tag{9}$$

and the dummy-suffix summation convention is employed with all summations ranging from 1 to n.

To study the path variation of the potential energy we have

$$V^{\mathrm{P}}(s) = V[u_i(s), \Lambda(s)], \tag{10}$$

and by differentiating repeatedly we obtain

$$V^{\mathrm{P}(1)} = V_i\, u^{(1)}_i + V'\Lambda^{(1)}, \tag{11}$$

$$V^{\mathrm{P}(2)} = [V_{ij}\, u^{(1)}_j + V'_i\, \Lambda^{(1)}]\, u^{(1)}_i + V_i\, u^{(2)}_i + [V'_i\, u^{(1)}_i + V''\Lambda^{(1)}]\, \Lambda^{(1)} + V'\Lambda^{(2)}, \tag{12}$$

etc.

Finally for the specialized P-system we can examine the path variation of the generalized deflexion

$$\mathscr{E}^{\mathrm{P}}(s) = \mathscr{E}^{\mathrm{P}}[u_i(s)] = -V'[u_i(s)] \tag{13}$$

by differentiating repeatedly as follows:

$$\mathscr{E}^{\mathrm{P}(1)} = -V'_i\, u^{(1)}_i, \quad \text{etc.} \tag{14}$$

4. *Normal equilibrium state*

We study first the variations through a normal, non-critical equilibrium state for which all the stability coefficients are non-zero:

$$V^{\mathrm{E}}_{ii} \neq 0 \quad \text{for all} \quad i. \tag{15}$$

For such a state it is permissible to identify our progress parameter s as the change in the control parameter so that

$$s = \lambda = \Lambda - \Lambda^{\mathrm{E}}, \tag{16}$$

and hence $$\Lambda^{(1)} = 1 \quad \text{while} \quad \Lambda^{(t)} = 0 \quad \text{for} \quad t \neq 1. \tag{17}$$

Evaluating the first equilibrium equation (7) at E we have, because $V^{\mathrm{E}}_{ij} = 0$ for $i \neq j$ as a result of employing principal coordinates,

$$V_{ii}\, u^{(1)}_i + V'_i|^{\mathrm{E}} = 0 \quad \text{(no summation)}, \tag{18}$$

giving $$u^{(1)\mathrm{E}}_i = -V'^{\mathrm{E}}_i / V^{\mathrm{E}}_{ii}. \tag{19}$$

The path variation of V at E is then, from (11),

$$V^{\mathrm{P}(1)\mathrm{E}} = V'^{\mathrm{E}} \tag{20}$$

since $V_i^{\mathrm{E}} = 0$, and the second variation is, from (12) with the use of (19),

$$V^{\mathrm{P}(2)\mathrm{E}} = V''^{\mathrm{E}} - \sum_{i=1}^{i=n} \frac{(V_i'^{\mathrm{E}})^2}{V_{ii}^{\mathrm{E}}}. \tag{21}$$

In terms of the conjugate parameter of equation (4), this result can be written

$$\left.\frac{\mathrm{d}K}{\mathrm{d}\Lambda}\right|^{\mathrm{E}} = \sum_{i=1}^{i=n} \frac{(V_i'^{\mathrm{E}})^2}{V_{ii}^{\mathrm{E}}} - V''^{\mathrm{E}} \tag{22}$$

and finally we can establish the path variation of $\mathscr{E}$ for the specialized P-system as

$$\left.\frac{\mathrm{d}\mathscr{E}^{\mathrm{P}}}{\mathrm{d}\Lambda}\right|^{\mathrm{E}} = \mathscr{E}^{\mathrm{P}(1)\mathrm{E}} = \sum_{i=1}^{i=n} \frac{(V_i'^{\mathrm{E}})^2}{V_{ii}^{\mathrm{E}}}. \tag{23}$$

Now if our basic equilibrium state E is vanishingly close to a fold so that V_{11}^{E} (say) is vanishingly small, and since it is a property of a fold or limit point that $V_1'^{\mathrm{E}}$ will not be vanishingly small (Thompson & Hunt 1973), we see that both of these total derivatives will be dominated by the term for which $i = 1$. They will thus both have the same sign as the vanishing stability coefficient V_{11}^{E} and our first two theorems are confirmed.

For our specialized system, equation (23) also gives us the global result, valid both near to and away from folds:

THEOREM 4. *The unique equilibrium path passing through a thoroughly stable equilibrium state cannot have a negative slope on a plot of the generalized force against its corresponding deflexion.*

Here 'thoroughly' signifies that all V_{ii}^{E} must be positive.

5. *Critical equilibrium state*

To examine the energy transformation in the fold more carefully, we shall now make a perturbation study at a fold or limit point C, for which

$$V_{11}^{\mathrm{C}} = 0 \quad \text{while} \quad V_{tt}^{\mathrm{C}} \neq 0 \quad \text{for} \quad t \neq 1. \tag{24}$$

Here, since Λ reaches an extreme value, we must take $s = u_1$, the critical principal coordinate.

Setting $i = 1$ in equation (7) we have on evaluation at C,

$$V_1'^{\mathrm{C}} \Lambda^{(1)\mathrm{C}} = 0, \tag{25}$$

and since for a limit point $V_1'^{\mathrm{C}} \neq 0$, we have

$$\Lambda^{(1)\mathrm{C}} = 0. \tag{26}$$

For $i = t \neq 1$, equation (7) now gives $$u_t^{(1)\mathrm{C}} = 0, \tag{27}$$

and setting $i = 1$ in the second equilibrium equation (8) we find

$$V_{111} + V_1' \Lambda^{(2)}|^{\mathrm{C}} = 0, \tag{28}$$

giving $$\Lambda^{(2)\mathrm{C}} = -V_{111}^{\mathrm{C}}/V_1'^{\mathrm{C}}. \tag{29}$$

This is the curvature of the equilibrium path on a plot of Λ against u_1, and in a similar manner we can find an explicit expression for the third derivative $\Lambda^{(3)C}$ by continuing this well behaved perturbation scheme.

We now have sufficient information about the equilibrium path through the limit point C, and with the use of these solutions the equations of the energy variation become, from (11) and (12), etc.,

$$V^{P(1)C} = 0, \tag{30}$$

$$V^{P(2)C} = V'^{C}\Lambda^{(2)C}, \tag{31}$$

$$V^{P(3)C} = V^{C}_{111} + 3V'^{C}_{1}\Lambda^{(2)C} + V'^{C}\Lambda^{(3)C}. \tag{32}$$

By using the result (29) the third derivative can conveniently be simplified to

$$V^{P(3)C} = -2V^{C}_{111} + V'^{C}\Lambda^{(3)C}. \tag{33}$$

Now, truncating the Taylor series for the change in V^P and the change in Λ, and noting that in each series the linear coefficient is zero, we have

$$v^P = \tfrac{1}{2}V^{P(2)C}u_1^2 + \tfrac{1}{6}V^{P(3)C}u_1^3, \tag{34}$$

$$\lambda = \tfrac{1}{2}\Lambda^{(2)C}u_1^2, \tag{35}$$

and substituting for u_1 we have

$$v^P = V'^{C}\lambda \pm \tfrac{1}{6}[-2V^{C}_{111} + V'^{C}\Lambda^{(3)C}][2\lambda/\Lambda^{(2)C}]^{\frac{3}{2}}. \tag{36}$$

Hence

$$v^P = V^P - V^{PC} = V'^{C}\lambda \pm B\lambda^{\frac{3}{2}}, \tag{37}$$

where B is a constant, and we notice that by adjusting the arbitrary energy data we could arrange that $V'^{C} = 0$, giving us simply

$$v^P = \pm \bar{B}\lambda^{\frac{3}{2}} \quad (\bar{B} \neq B). \tag{38}$$

This is the cusp-like energy variation of figure 1, and on differentiation we have

$$K(\Lambda) = -\mathrm{d}V^P/\mathrm{d}\Lambda = -V'^{C} \mp \tfrac{3}{2}B\lambda^{\frac{1}{2}}, \tag{39}$$

giving us the parabolas of figure 2.

Analytical proofs of our theorems follow in a straight-forward manner from this critical state analysis, but we shall not pursue them here.

II. The concept of internal stability

6. *Extreme forms of loading*

We consider a conservative elastic structure or component, suitably discretized, subjected to a single generalized load. Such a load might be associated with a number of discrete forces or even a distributed pressure by the use of links, hydraulic pistons, etc. (Thompson 1961).

This generalized load will usually be dead under service conditions, in the sense that the magnitude of the force P is a controlled quantity. Examples are provided by masses in a gravitational field, or static fluid forces on an immersed body.

Experimentally, however, it is advantageous to test model structures under some form of rigid loading, ideally by imposing values of the corresponding deflexion $\mathscr{E}$. Then, having determined the behaviour of a structure in a rigid testing machine it is pertinent to ask the question: 'What now would be the behaviour of the structure under the dead loading of more practical conditions?

We aim to answer this question in general terms for our previously defined P-system of equation (1) and, following the apt terminology of Ashwell (1962), we shall speak of the *external* stability of a structure under *dead* loading and conversely the *internal* stability under *perfectly rigid* loading.

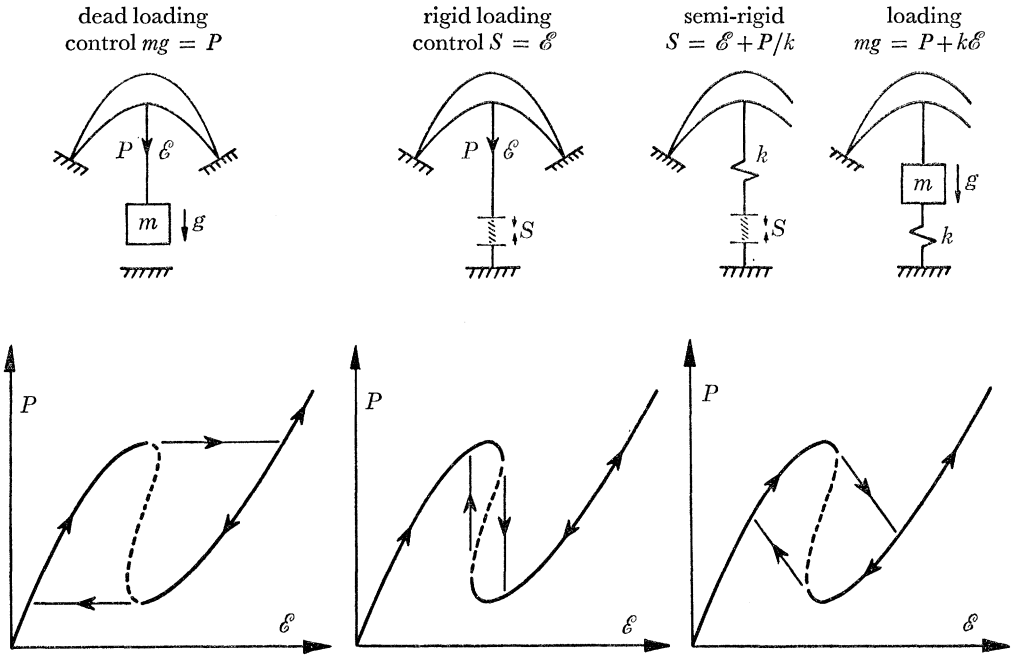

FIGURE 5. Folds and hysteresis cycles in the loading of an elastic structure.

7. *Practical loading arrangements*

While it is usually easy to ensure dead loading of a structural model, it is of course impossible without resort to a complicated control system to impose a strict value of the corresponding deflexion due to the inherent elasticity of any testing frame. We are then lead to consider the four situations of figure 5.

In the first arrangement we have dead loading by the imposition of $P = mg$ which is our control parameter with the energy function of equation (1), $V(Q_i) = U(Q_i) - P\mathscr{E}(Q_i)$. Fold catastrophes arise at extreme values of P and dynamic snaps will be at constant P as indicated.

In the second arrangement we have *idealized* rigid loading by the imposition of $\mathscr{E} = S$ where S is the contraction of a perfectly rigid screw device. The corresponding deflexion $\mathscr{E}$ is now our control parameter; folds arise at extreme values of $\mathscr{E}$ and dynamic snaps will be at constant $\mathscr{E}$ as illustrated.

The third arrangement shows a practical approach to rigid loading with a spring of stiffness k representing the elasticity of the whole testing device. This spring plus the perfectly rigid screw represents a valid model of the majority of *semi-rigid* loading devices. Our control parameter is S which is equal to $\mathscr{E} + P/k$, so that we have inclined loading lines in the load–deflexion diagram, fold catastrophes occurring where these lines touch the equilibrium path of the structure and dynamic jumps being forced to follow the current loading line as shown.

The fourth arrangement shows another commonly employed form of semi-rigid loading. Here mg is our control and since $mg = P + k\mathscr{E}$ we are again imposing inclined loading lines as shown; and analytically this arrangement is identical to that of the previous case.

Conceptually these two practical semi-rigid loading devices can be viewed as 'structure plus spring' under rigid loading and 'structure plus spring' under dead loading, so that our present discussions of dead and perfectly rigid loading will effectively cover the problems of semi-rigid loading. Theorem 4, for example, which implies that if the slope of the load–deflexion curve of a structure is negative, then the structure must be unstable under dead loading, tells us that for semi-rigid loading we have the result:

THEOREM 5. *If the sum of the slopes of the load–deflexion characteristics of the structure and its testing machine is negative, then the system is unstable.*

A more general loading system can of course be imagined in which a family of straight or curved loading lines is simply prescribed, as discussed in an earlier paper (Thompson 1961).

8. *The conjugate property*

Under dead loading, with $\mathrm{P} = \Lambda$ as the control and the relevant energy function given by equation (1), the path variation of V at a normal equilibrium state E is

$$\mathrm{d}V^{\mathrm{P}}/\mathrm{d}\Lambda = V_i u_i^{(1)} + V' \tag{40}$$

with the progress parameter s equated to the change in Λ, so evaluating at E we have

$$\mathrm{d}V^{\mathrm{P}}/\mathrm{d}\Lambda|^{\mathrm{E}} = V'^{\mathrm{E}} = -\mathscr{E}. \tag{41}$$

Thus the conjugate parameter K is equal to $\mathscr{E}$ as we have seen in theorem 2.

Under rigid loading, $\mathscr{E}$ becomes our control parameter and to apply the general theory of elastic stability or catastrophe theory in their direct forms we must make a change of coordinates. We replace the original n generalized coordinates Q_i by a set of $n-1$ coordinates X_i which, together with $\mathscr{E}$, describe uniquely the deformed state of the structure. The strain energy is then a single-valued function of the X_i and $\mathscr{E}$, $U = U(X_i, \mathscr{E})$, and this becomes the relevant energy function.

Now, for a small displacement along an equilibrium path we have the condition $\delta U = P\delta\mathscr{E}$ so that

$$P = \mathrm{d}U^{\mathrm{P}}/\mathrm{d}\mathscr{E}. \tag{42}$$

Thus the negative of P is now equal to the conjugate parameter K as we have seen in theorem 3.

9. *Relations between internal and external stability*

The direct treatment of internal stability, while indicating the behaviour of a structure under an imposed displacement, is essentially distinct from the direct treatment of the same structure under an imposed load due to the change of coordinates. Consequently it is instructive to study the problem of internal stability again, now with the use of the original Q_i coordinate system of the dead load analysis. This will allow some vital interrelation to be established.

Equilibrium states under rigid loading are now defined by the stationarity of $U(Q_i)$ under the constraint of constant $\mathscr{E}$. The states are of course the same as those that arise in the dead load analysis, as is transparent by the use of a Lagrange multiplier which plays the role of the force magnitude P.

To investigate the stability of an equilibrium state under rigid loading we must now study the second variation of $U(Q_i)$ with the constraint of constant $\mathscr{E}$. Clearly however we are free to study the second variation of the dead load energy function, $V = U - P\mathscr{E}$, with the same restraint. Thus

while the external stability of an equilibrium state E is determined by the second variation of V,

$$\delta^2 V = \frac{1}{2} \sum_{i=1}^{i=n} V_{ii}^{\mathrm{E}} u_i^2, \tag{43}$$

which we write more simply as

$$Z = \tfrac{1}{2} C_i u_i^2, \tag{44}$$

the internal stability will be determined in the first instance by the same expression with the linear constraint

$$\delta \mathscr{E} = \mathscr{E}_i^{\mathrm{E}} u_i = 0, \tag{45}$$

which we write more simply as

$$Y = S_i u_i = 0. \tag{46}$$

Two results are immediately seen. If the structure is stable under dead loading, so that all the stability coefficients C_i are positive, the structure must be stable under rigid loading. Secondly, if the structure has two or more degrees of instability under dead load (so that two or more of the C_i are negative) then it is unstable under rigid loading; this conclusion follows immediately from a result of Courant & Hilbert (1953). Thus the only case of further interest arises when a single dead load stability coefficient is negative.

We proceed to determine the $n-1$ stationary values of Z on the 'sphere'

$$\sum_{i=1}^{i=n} u_i^2 = 2 \tag{47}$$

with the constraint $Y = 0$. Without the constraint, the n stationary points of Z occur on the principal u_i axes, to give the dead load stability coefficients $Z = C_1$, $Z = C_2$, ..., $Z = C_n$. With the constraint, the stationary values will represent a set of $n-1$ rigid load stability coefficients.

With the introduction of two Lagrange multipliers, $\frac{1}{2} r_1$ and r_2, we consider the auxiliary problem of locating the stationary points of

$$\bar{Z} = \tfrac{1}{2} \Sigma C_i u_i^2 - \tfrac{1}{2} r_1 [\Sigma u_i^2 - 2] - r_2 \Sigma S_i u_i. \tag{48}$$

The subsequent analysis is presented in detail in the Appendix, and the required stationary values of Z are given by the $n-1$ values of r_1 satisfying the equation

$$\Sigma \frac{S_i^2}{(C_i - r_1)} \Big/ \left(\Sigma \frac{S_i^2}{(C_i - r_1)^2} \right)^{\frac{1}{2}} = 0 \tag{49}$$

which can in general be simplified by omitting the denominator.

Thus a set of stability coefficients for rigid loading is given by the $n-1$ roots of (49), and for a change of internal stability this equation must be satisfied by $r_1 = 0$. Thus the general condition for a change of internal stability can be written as

$$\Sigma S_i^2 / C_i = \sum_{i=1}^{i=n} \frac{(V_i'^{\mathrm{E}})^2}{V_{ii}^{\mathrm{E}}} = 0. \tag{50}$$

Comparison of this with equation (23) confirms our direct prediction that internal stability is normally lost at a fold involving an extremum of the deflexion $\mathscr{E}$.

The fact that a structure cannot be internally unstable when externally stable clearly poses limitations on the form of the equilibrium paths of our P-system: a rigid load fold must for example be encountered *after* a dead load fold as we have illustrated in figure 5.

If one of the S_i coefficients (S_1 say) is zero, the numerator of (49) loses one of its roots, and the missing solution supplied by the complete equation is $r_1 = C_1$ assuming all the C_i to be distinct.

Now the simultaneous vanishing of S_1 and C_1 gives us a point of bifrucation (Thompson & Hunt 1973) and so we can infer that the fundamental path of a distinct point of bifurcation beyond the branch cannot be stabilized by rigid loading. This result is established more rigorously by a non-linear discussion in part III, and corresponds to the fact that with $S_1 = 0$ the constraint is orthogonal to the incipient instability.

10. *Internal stability with external instability*

An equilibrium state of a structure might be internally and externally stable, or internally and externally unstable. The only other possibility, since internal instability implies external instability, is that the state is internally stable but externally unstable, and we shall now examine the conditions under which this last possibility can be realized.

Restricting attention to a perfectly general *non-critical* equilibrium state, let us suppose that $\bar{r}_1$, the smallest root of

$$\Sigma S_i^2/(C_i - r_1) = 0 \tag{51}$$

is positive, so that the basic state is internally stable. Then if we suppose that $C_1 < C_2 < C_3 \ldots < C_n$, it follows from a result of Courant & Hilbert (1953) that $C_1 < \bar{r}_1 < C_2$. Thus C_s must be positive for s not equal to one, while C_1 may be positive or negative.

Let us suppose that C_1 is negative, and consider the two series

$$\Sigma S_i^2/(C_i - \bar{r}_1) = 0 \quad \text{and} \quad \Sigma S_i^2/C_i. \tag{52}$$

We see that in each series the first term is negative, and the remaining terms are positive. Moreover in changing from a term in the first series to the corresponding term in the second series the negative term has increased in absolute magnitude while the following positive terms have all decreased in magnitude. Clearly the sum of the second series must be negative.

Thus if $\bar{r}_1$ is positive and C_1 is negative, the slope of equation (23) must be negative: moreover if C_1 is positive it is clear that the slope will be positive.

It follows that if an equilibrium state of a structure is internally stable it will also be externally stable unless the equilibrium path passing through that state has a negative slope on a plot of the load against the corresponding deflexion. That is to say a state of internal stability and external instability will always be associated with a negative slope on a plot of P against $\mathscr{E}$.

When applied to semi-rigid loading this gives us the result:

THEOREM 6. *If the sum of the slopes of the load–deflexion characteristics of the structure and its testing machine is positive, then the system is stable provided both the structure and machine are themselves internally stable.*

This theorem states that the converse of theorem 5 is true provided the structure and machine are internally stable.

III. APPLICATIONS

11. *A pinned arch*

To illustrate the application of our theorems we consider first the shallow pinned arch or curved beam shown in figure 6. It carries a concentrated load at its vertex, and for deformations symmetrical about its centre line Biezeno & Grammel (1960) determine theoretically the single continuous equilibrium path shown. This path exhibits no branching points, the curve simply

appearing to cross itself on this projection, and similar equilibrium paths have been obtained more recently by Harrison (1978).

Using theorem 2 for dead loading we can deduce that as we move from the stable origin we have two losses of stability followed by two gains as indicated. In the figure L indicates a loss and G a gain; a solid circle denotes a stable equilibrium state, a half-solid circle denotes a state with one degree of instability and an open circle denotes a state with two degrees of instability. Thus under dead loading the arch would jump dynamically from the first fold to the final stable state as indicated by the snap arrow.

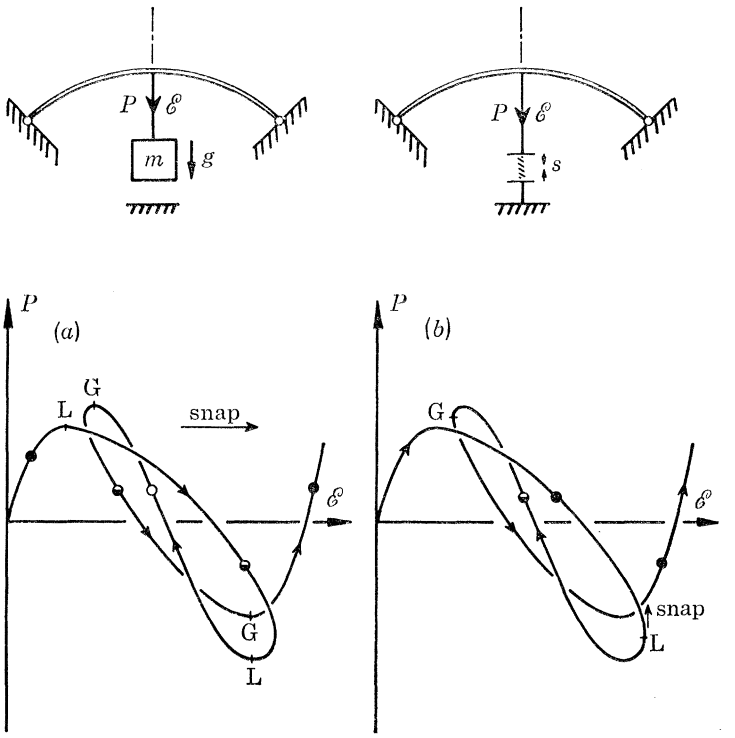

FIGURE 6. A pinned elastic arch under (*a*) dead and (*b*) rigid loading. A solid circle denotes zero, a half-solid circle denotes one and an open circle denotes two degrees of instability.

Using theorem 3 for rigid loading we can likewise infer one loss and one gain of internal stability, as indicated in the right-hand graph, with an initial snap during which the passive constraining force P actually increases. A superb experimental study of this due to Croll & Walker (1972) is shown in figure 7, the arch being here constrained to deform symmetrically throughout by means of a central plunger. The mode forms before and after the original dynamic snap are indicated, the value of the central deflexion, d, being held essentially constant during the motion by the very stiff semi-rigid loading device.

12. *A shallow spherical dome*

Consider secondly the elastic structure of figure 8. A shallow spherical dome of uniform thickness is loaded at the apex by a concentrated force P and is freely supported at the circumference. The rotationally-symmetric deformations of the dome are analysed by Biezeno & Grammel (1960), and for a certain shell geometry the load–deflexion curves are as shown. The continuous curve from the origin represents a typical shallow shell snapping response, the curve having the

unusual feature of a second relative maximum. The isolated loop is a feature of many problems of this nature. The paths do not coincide at any of the apparent intersections on the P–$\mathscr{E}$ graph, so there are no branching points present.

Using theorem 2 for dead loading we can deduce that as we progress from the origin we encounter a loss, a gain, a loss and a final gain of stability as indicated. The degree of instability of the curve can thus be everywhere assessed, and a dynamic snap would be observed from the first fold to the finally heavily deflected state.

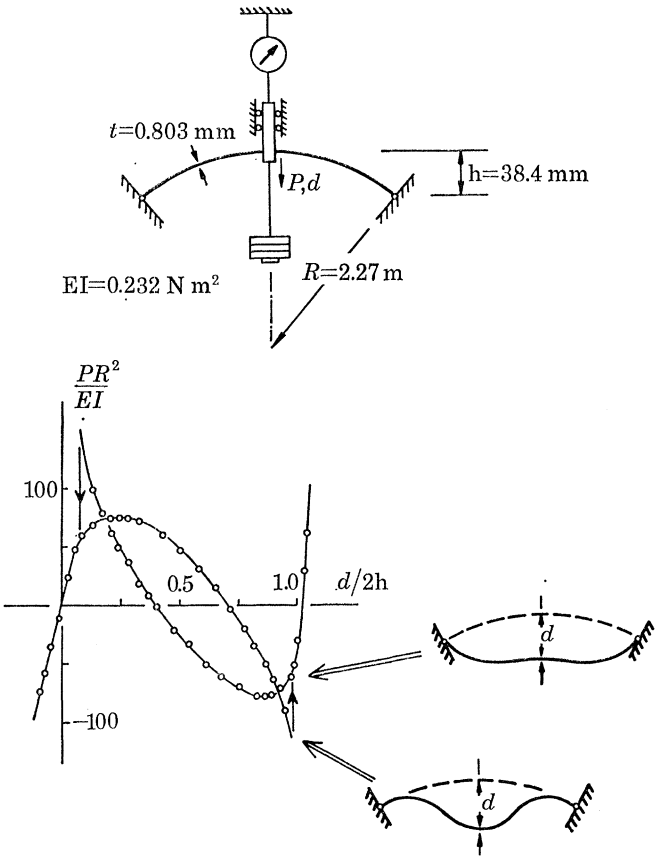

FIGURE 7. An experimental study of the symmetric deformations of a pinned arch under very rigid loading, due to Croll & Walker (1972).

Using theorem 3 for rigid loading we have no folds on the path from the origin which is thus everywhere internally stable. No dynamic snap would be encountered under rigid loading.

The closed loop requires a separate discussion. As the loop is traversed in the direction of the arrows the losses and gains of internal and external stability can be deduced as shown: but since there is no state of known stability on the loop the precise degree of instability cannot be deduced by the use of these two theorems alone.

We can note finally that a closed loop of this type must of necessity enclose zero net area for a conservative system.

13. *Thermodynamics of a hot stellar mass*

In his original application of theorem 1, Katz (1978) considers the stability of hot stellar spheres with identical particles. For this thermodynamical problem a graph of the inverse of the

temperature, T^{-1}, against the energy, E, serves to identify all the stability transformations for two distinct situations. A vertical tangent defines a stability change for an isolated star, while a horizontal tangent defines a stability change for a star in a heat bath.

The conjugate properties of T^{-1} and E clearly have a profound similarity to the conjugate properties of P and $\mathscr{E}$ in our discussion of dead and rigid loading.

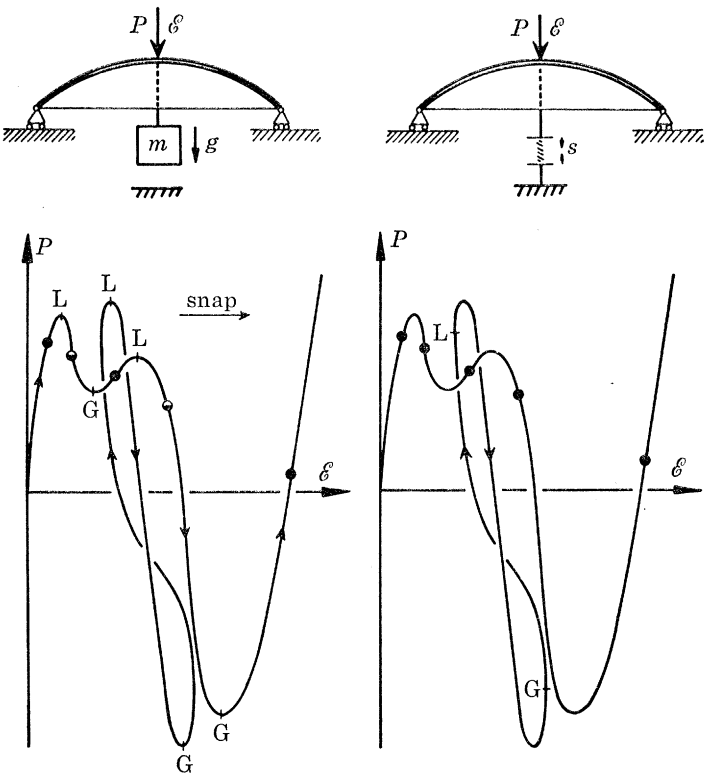

FIGURE 8. A shallow spherical dome under (*a*) dead and (*b*) rigid loading.

14. *Gravitational collapse of a massive cold star*

To shed some light on the realistic gravitational collapse of a massive hot star, which would include the complications of angular momentum, magnetic fields, turbulence and shock waves, Harrison *et al.* (1965) considered the ground state of a system of A baryons, neutrons and protons, that have been catalysed to the end point of thermonuclear evolution and cooled as closely as desired to absolute zero.

For $A = 1$ the ground state corresponds to one hydrogen atom, for $A = 4$ to a helium atom and for $A = 56$ to an iron atom. Stepping up to $A = 56 \times 10^6$ the catalysed end product is a set of 10^6 iron atoms, ^{56}Fe, arranged in a body-centred cubic lattice. When the baryon number reaches the order of 10^{56} or 10^{57} the self-induced gravitational forces are so powerful that the extreme pressure raises the electrons to relativistic energies and they transmute protons to neutrons. The nuclear composition changes from ^{56}Fe to heavier and more neutron-rich nuclei.

Using the unique and universal equation of state corresponding to this cold catalysed matter, an analysis is made of the spherically symmetric equilibrium configurations of a self-gravitating stellar mass, the necessary general relativistic equation of hydrostatic equilibrium being obtained by extremizing the mass as sensed externally. The stability of these equilbrium configurations

against radial spherically symmetric disturbances is determined by studying the characteristic acoustical modes of vibration and by examining the second variation of the mass energy for a fixed baryon number.

The results of these equilibrium and stability analyses are summarized in figure 9 the top graph being a plot of the mass energy against the central density. We see that there are only two regions of stability corresponding to white dwarf stars and neutron stars respectively. With an increasing number of baryons and mass energy, each of these regions terminates at a critical equilibrium state corresponding to a fold catastrophe at which gravitational forces dominate and collapse can start. We note in particular that the critical masses, M, are of the order of the mass of the sun, $M_\odot$, and that the critical equilibrium states beyond C all represent a further destabilization of the stellar system.

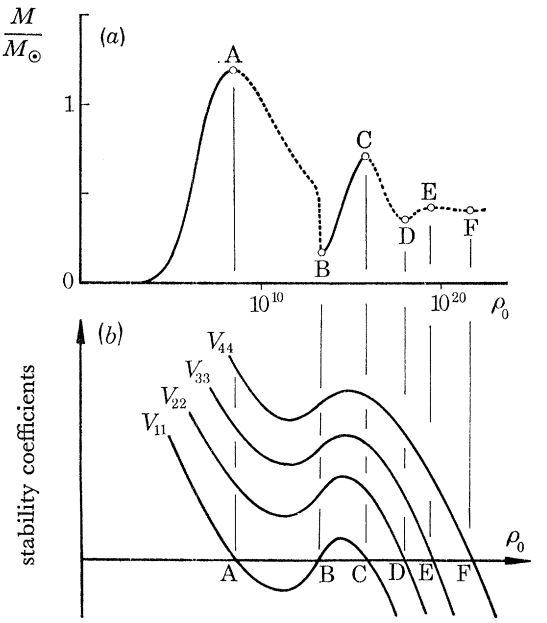

FIGURE 9. Equilibrium and stability of a massive star compressed by its own gravitational field. (*a*), The mass energy as a fraction of the solar mass against the central density in g/cm^3; (*b*), the variation of the acoustical stability coefficients.

As the equilibrium path emerges from the vicinity of the origin we start with an atom of hydrogen, a cannon ball of iron, objects of planetary mass and finally the cold white dwarfs. The first instability at the fold A, which can be predicted by using only a Newtonian equilibrium equation, corresponds to the overwhelming of the electron pressure at a baryon number of approximately 1.4×10^{57}. At the minimum B the stellar matter has been crushed to a substantial fraction of nuclear density and its increased rigidity leads to the stable neutron stars. At the second peak C the gravitational forces finally dominate even this nuclear rigidity. We note here that the baryon number at C, 0.84×10^{57}, is lower than that at A. Therefore, if in a highly idealized dynamical collapse of a cold white dwarf there was no change in the baryon number (no matter thrown off), the star could not stabilize as a neutron star.

The complete stability analysis for spherically symmetric disturbances due to Harrison *et al.* (1965) forms a most attractive illustration of our general analysis. They identified the mass energy M as a governing *potential* determining both the equilibrium and stability, with the baryon

number A (or equivalently the mass before assembly M_A which is proportional to A) playing the role of a *control parameter* and the central density ρ_0 playing the role of an active *generalized coordinate*. They drew a three dimensional picture of the energy transitions in the M–A–ρ_0 space exactly equivalent to our figure 1 of the fold catastrophe with $\partial M/\partial A = V'^{\mathrm{C}} \neq 0$ at the critical point. Under this condition they observed that both the potential M and the control A took extreme values on the equilibrium path at the critical point, and they demonstrated the two-thirds power law cusp in the energy–control projection.

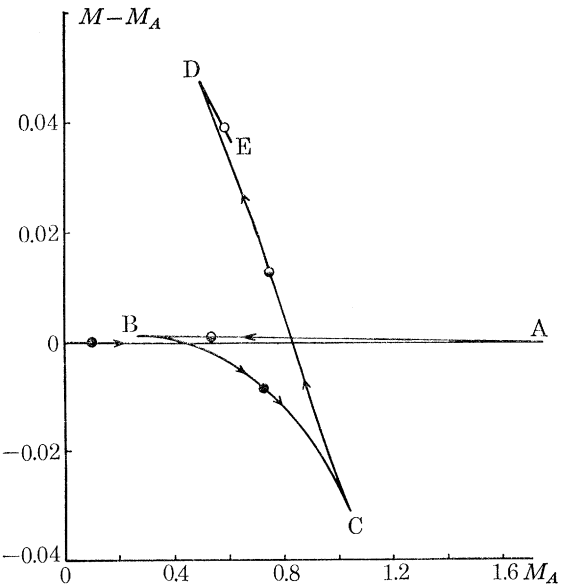

FIGURE 10. The energy versus control cusps for the folds of a massive star on a plot of the mass energy minus the mass before assembly, $M-M_A$, against the mass before assembly, M_A. A solid circle denotes zero, a half-solid circle denotes one, and an open circle denotes two degrees of instability.

Now the mass before assembly, M_A, is simply the baryon number A multiplied by the standard baryon mass μ_S and so represents a valid control parameter. It is however closely equal to the equilibrium mass energy M, and for this reason the projection of the equilibrium path onto the energy–control plane lies very close to the 45° line. To observe the cusps it is therefore more convenient to plot M minus M_A (which is of course also a valid potential function) against the control M_A and we have done this in figure 10. On this picture, by inspecting the energy levels close to the folds, we can deduce the sequence of stability transformations shown in the lower graph of figure 9.

At A the originally stable path loses its stability with respect to mode one by the passage through zero of the first stability coefficient V_{11}. Stability is recovered at B by the passage back through zero of V_{11} but finally lost at C as this stability coefficient again becomes negative. Each fold after C now corresponds to a loss of stability, V_{22} becoming negative at D, V_{33} becoming negative at E, V_{44} becoming negative at F, etc.

These statical computations and the associated linear vibration analyses form an attractive illustration of a sequence of fold catastrophes, and the slow gravitational capture of mass by a white dwarf or neutron star gives us the slow evolutionary change of the control parameter. However, once collapse is initiated at A or C most of the assumptions of the highly idealized

analysis break down. Both baryons and radiant energy may be lost from the system (Weinberg 1972, Misner *et al.* 1973) and so the value of the control parameter is not preserved.

Questions such as the possible formation of a black hole by the collapsing star are thus quite beyond the scope of this idealized study.

We must finally comment on the close numerical equivalence of M_A and M on the equilibrium path. This has caused some misunderstanding in the past. From a conceptual point of view the distinction is clear and vital, as has been emphasized by E. C. Zeeman (1977 in private correspondence with the author): the mass *before assembly*, M_A, is the catastrophe theory *control* parameter while the mass *after assembly*, M, is the catastrophe theory *potential*. However, when we have solved the equilibrium equations and come to plot the equilibrium values of M and M_A against the generalized coordinate ρ_0 we shall find that the two graphs are for all practical purposes identical. To illustrate this point we show in table 1 the ratio of M to M_A at the critical points where it departs furthest from unity, and we see that the equilibrium graphs could not easily be distinguished.

TABLE 1

	M/M_A
first maximum A	0.9999
first minimum B	1.0041
second maximum C	0.9701
second minimum D	1.0980
third maximum E	1.0603

15. *Bifurcations under rigid loading*

A basic theorem of elastic stability (Thompson 1970; Thompson & Hunt 1973) recently proved by Kuiper, as reported by Chillingworth (1976), ensures that in the absence of a fold, the initial stability of a discrete conservative system under a single control parameter can only be lost at a point of bifurcation. Such a branching point is of course structurally unstable (Thom 1975) but is nevertheless of considerable theoretical relevance, and we shall now apply some of our results to assess the corresponding *internal* stability changes for our specialized P-system.

A useful trick in determining the stability transformations at a point of bifurcation is to examine the adjacent equilibrium paths of imperfect systems which generically only exhibit folds, since the stability of perfect and imperfect states will be identical as the imperfection magnitude is allowed to vanish. The validity of this argument becomes apparent when the full equilibrium surfaces are inspected (Thompson & Hunt 1975, Hunt 1977).

We have used this procedure to examine the internal stability changes for a specialized P-system exhibiting the three distinct branching points classically delineated by Koiter (1945). These are shown in figure 11 on a plot of the generalized load P against a typical Q_i coordinate and on the special P against $\mathscr{E}$ plot. Determination of the changes of *internal* stability by the folds in the response of imperfect systems allows us to establish completely the stability changes shown, a solid curve denoting a path that is internally stable under prescribed $\mathscr{E}$ and a broken curve denoting a path that is internally unstable under prescribed $\mathscr{E}$. The folds of imperfect systems that correspond to extreme values of the corresponding deflexion $\mathscr{E}$ are drawn as small circles.

We see that for the perfect systems the only difference between these pictures and the well-known dead-load stability diagrams is that the post-buckling path of the unstable–symmetric point of bifurcation is stabilized by rigid loading if its slope is negative on the P against $\mathscr{E}$ plot.

PHILOSOPHICAL TRANSACTIONS OF THE ROYAL SOCIETY A MATHEMATICAL, PHYSICAL & ENGINEERING SCIENCES

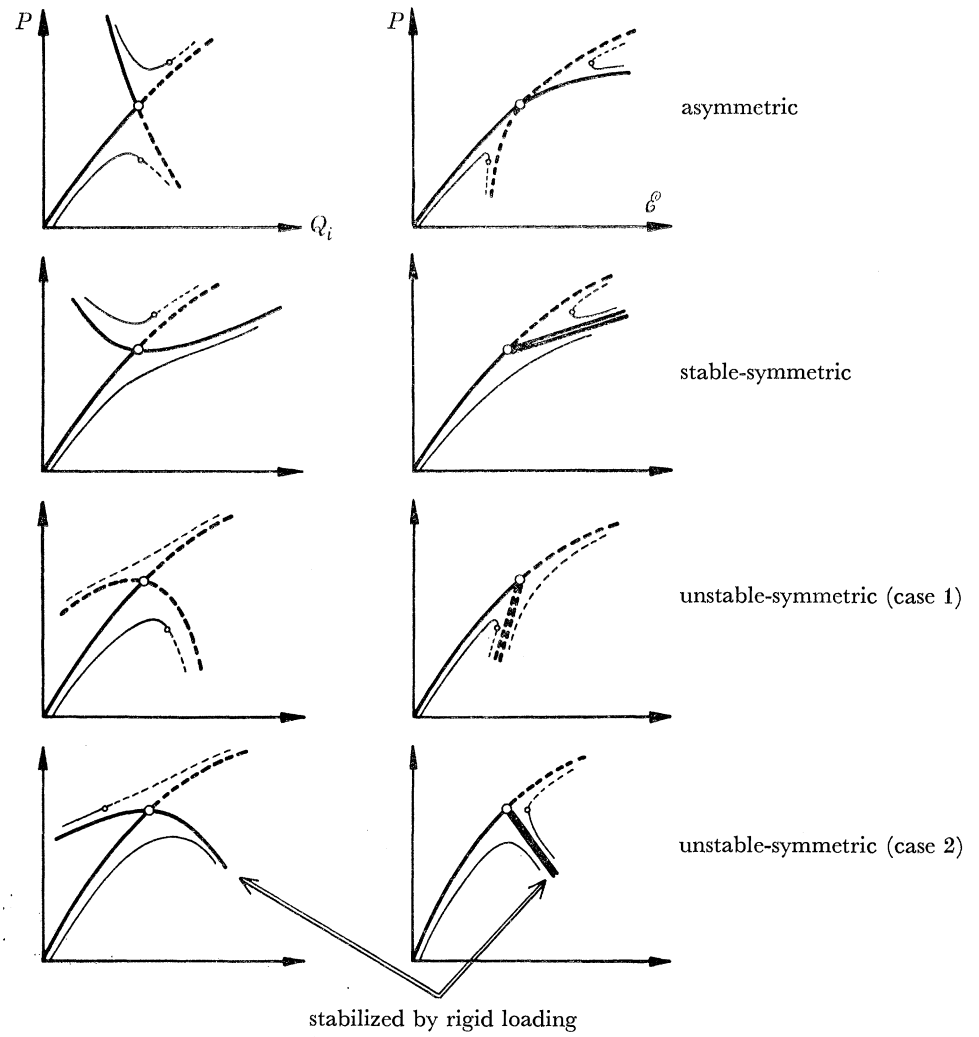

FIGURE 11. Changes of *internal* stability at distinct branching points. Solid lines denote states that are stable under rigid loading while broken lines denote states that are unstable under rigid loading.

CONCLUDING REMARKS

Fold catastrophes, in their own right, and in the perturbations of branching points, play a central role in the theory of generic instabilities (Thom 1975, Zeeman 1977, Poston & Stewart 1978, Thompson & Hunt 1977). This importance is emphasized by their being the only structurally stable singularities that can be observed in the real world during the operation of a single control parameter. We have shown that the conjugate theorem and the more specialized theorems established for the internal and external stabilities of an elastic structure can be useful in assessing the stability transitions through a succession of folds and, indirectly, the stability changes at bifurcations.

Appendix

The evaluation of the stationary values of

$$Z = \tfrac{1}{2}\Sigma C_i u_i^2$$

on the 'sphere' $\Sigma u_i^2 = 2,$

with the constraint $\Sigma S_i u_i = 0,$

is here presented in detail. In this way the range of validity of the 'general' results quoted in section 9 is made apparent.

To determine the stationary values of Z we introduce the two Lagrange multipliers, $\frac{1}{2}\rho_1$ and ρ_2, and consider the auxiliary function

$$\bar{Z} = \tfrac{1}{2}\Sigma C_i u_i^2 - \tfrac{1}{2}\rho_1(\Sigma u_i^2 - 2) - \rho_2 \Sigma S_i u_i.$$

The stationary points of this function are also the stationary points of Z, so for the stationary values we must evaluate Z under the conditions

$$\Sigma u_i^2 = 2, \tag{A}$$

$$\Sigma S_i u_i = 0, \tag{B}$$

and $$\partial \bar{Z}/\partial u_r = C_r u_r - \rho_1 u_r - \rho_2 S_r = 0 \quad \text{for all} \quad r. \tag{C}$$

We can observe that these conditions represent $n+2$ equations for the $n+2$ 'unknowns' u_i, ρ_1 and ρ_2.

If we multiply the rth equation of C by u_r, repeating this procedure for all values of r from 1 to n, and then sum the resulting n equations, we have

$$\Sigma C_i u_i^2 - \rho_1 \Sigma u_i^2 - \rho_2 \Sigma S_i u_i = 0.$$

Now, by using equations (A) and (B) this yields

$$Z = \tfrac{1}{2}\Sigma C_i u_i^2 = \rho_1.$$

Thus the evaluation of the stationary values of Z reduces to the solution of equations (A), (B) and (C) for ρ_1.

Equation (C) gives $$u_r = \rho_2 S_r/(C_r - \rho_1) \quad \text{for all} \quad r.$$

Substitution of this expression for u_r in equation (A) gives

$$\rho_2^2 \Sigma S_i^2/(C_i - \rho_1)^2 = 2, \tag{D}$$

and substitution of the expression for u_r in equation (B) gives

$$\rho_2 \Sigma S_i^2/(C_i - \rho_1) = 0. \tag{E}$$

Finally eliminating ρ_2 (which might of course be zero) from these two equations we have the single equation for ρ_1,

$$\Sigma \frac{S_i^2}{C_i - \rho_1} \Big/ \left(\Sigma \frac{S_i^2}{(C_i - \rho_1)^2}\right)^{\frac{1}{2}} = 0. \tag{F}$$

The $n-1$ roots of this equation will supply the required stationary values of Z. We shall write $\rho_1 = \bar{\rho}_1$ to represent a particular solution of the equation.

Considering the evaluation of a particular solution, and with a view to dropping the

denominator from the left-hand side, let us examine the conditions under which the denominator of equation F can become infinite.

We shall assume that all the coefficients C_i are distinct, so that $C_i \neq C_j$ for all $i \neq j$. Clearly then the denominator can only tend to infinity if $\bar{\rho}_1$ tends to one of the coefficients C_i, C_1 say. Moreover S_1 must be of an order greater than $C_1 - \bar{\rho}_1$, so that $(C_1 - \bar{\rho}_1)/S_1$ is tending to zero.

Assuming then that $\bar{\rho}_1 \to C_1$ and $S_1 \gg (C_1 - \bar{\rho}_1)$, only the first term of the denominator need be retained, and equation (F) implies that

$$\frac{C_1 - \bar{\rho}_1}{S_1}\left(\frac{S_1^2}{C_1 - \bar{\rho}_1} + \frac{S_2^2}{C_2 - \bar{\rho}_1} + \ldots\right) = 0.$$

Considering now the first term in the brackets, we see that this equation implies that S_1 must be tending to zero.

Thus the only solutions that the denominator can supply are represented by $\bar{\rho}_1 = C_r$, which arises when S_r is equal to zero.

It follows that if no coefficient S_i is equal to zero, and if all the coefficients C_i are distinct, we can omit the denominator and write

$$\Sigma S_i^2/(C_i - \rho_1) = 0 \tag{G}$$

The roots of this equation will in general yield the $n-1$ stationary values of Z.

If however one of the coefficients S_i drops to zero, this equation loses one of its roots, and we have seen that the missing solution is supplied by the denominator of equation (F). More specifically, if p of the S_i, $S_1, S_2, \ldots, S_p$, are equal to zero, equation (G) will supply $n-1-p$ stationary values of Z, and the missing solutions will be given by $\rho_1 = C_1, \rho_1 = C_2, \ldots \rho_1 = C_p$, provided that all the C_i are distinct.

If one of the stationary values of Z is to be equal to zero, equation (F) must be satisfied by $\rho_1 = 0$. Thus the condition for a vanishing stationary value can be written as

$$\Sigma \frac{S_i^2}{C_i} \Big/ \left(\Sigma \frac{S_i^2}{C_i^2}\right)^{\frac{1}{2}} = 0 \tag{H}$$

If, moreover, no C_i is equal to zero, the denominator can be omitted, so that we have

$$\Sigma S_i^2/C_i = 0, \tag{I}$$

which is the 'general' condition for a vanishing stationary value of Z.

References

Ashwell, D. G. 1962 Nonlinear problems, Chapter 45, *Handbook of engineering mechanics*, (ed. W. Flugge). New York: McGraw Hill.

Biezeno, C. B. & Grammel, R. 1960 *Engineering dynamics*, Vol 2. London: Blackie.

Chillingworth, D. R. J. 1976 A problem from singularity theory in engineering. Lecture to Symposium on Nonlinear Mathematical Modelling, University of Southampton.

Courant, R. & Hilbert, D. 1953 *Methods of mathematical physics*, Vol. 1, p. 33. New York: Interscience.

Croll, J. G. A. & Walker, A. C. 1972 *Elements of structural stability*. London: Macmillan.

Harrison, B. K., Thorne, K. S., Wakano, M. & Wheeler, J. A. 1965 *Gravitation theory and gravitational collapse*. Chicago: University Press.

Harrison, H. B. 1978 Post-buckling behaviour of elastic circular arches. *Proc. Inst. civ. Engrs*, Part 2, **65**, 283–298.

Hunt, G. W. 1977 Imperfection-sensitivity of semi-symmetric branching. *Proc. R. Soc. Lond.* A **357**, 193–211.

Katz, J. 1978 On the number of unstable modes of an equilibrium. *Mon. Not. R. astr. Soc.* **183**, 765–769.

Koiter, W. T. 1945 On the stability of elastic equilibrium. Dissertation, Delft, Holland. (English translation: *N.A.S.A. tech. Trans.* F **10**, 1–833, 1967.)
Misner, C. W., Thorne, K. S. & Wheeler, J. A. 1973 *Gravitation*. San Francisco: Freeman.
Poston, T. & Stewart, I. 1978 *Catastrophe Theory and its Applications*. London: Pitman.
Thom, R. 1975 *Structural Stability and Morphogenesis*, (translated from the French by D. H. Fowler). Reading: Benjamin.
Thompson, J. M. T. 1961 Stability of elastic structures and their loading devices. *J. mech. Engng Sci.* **3**, 153–162.
Thompson, J. M. T. 1970 Basic theorems of elastic stability. *Int. J. engng Sci.* **8**, 307–313.
Thompson, J. M. T. & Hunt, G. W. 1973 *A General Theory of Elastic Stability*. London: Wiley.
Thompson, J. M. T. & Hunt, G. W. 1975 Towards a unified bifurcation theory. *Z. angew. Math. Phys.* **26**, 581–603.
Thompson, J. M. T. & Hunt, G. W. 1977 The instability of evolving systems. *Interdiscip. Sci. Rev.* **2**, 240–262.
Weinberg, S. 1972 *Gravitation and cosmology: principles and applications of the general theory of relativity*. New York: Wiley.
Zeeman, E. C. 1977 *Catastrophe theory: selected papers* 1972–1977. London: Addison Wesley.

PHILOSOPHICAL TRANSACTIONS OF THE ROYAL SOCIETY A MATHEMATICAL, PHYSICAL & ENGINEERING SCIENCES